Voter models with conserved dynamics

Voter models with conserved dynamics

Fabio Caccioli,[1,*] Luca Dall'Asta,[2,3,†] Tobias Galla,[4,‡] and Tim Rogers[5,§]
[1]*Santa Fe Institute, Hyde Park Road, Santa Fe, New Mexico 87501, USA*
[2]*DISAT and Center for Computational Sciences, Politecnico di Torino, Corso Duca degli Abruzzi 24, 10129 Torino, Italy*
[3]*Collegio Carlo Alberto, Via Real Collegio 30, 10024 Moncalieri, Italy*
[4]*Theoretical Physics, School of Physics and Astronomy, The University of Manchester, Manchester M139PL, United Kingdom*
[5]*Department of Mathematical Sciences, University of Bath, Claverton Down, Bath BA27AY, United Kingdom*
(Received 8 August 2012; revised manuscript received 28 February 2013; published 10 May 2013)

We propose a modified voter model with locally conserved magnetization and investigate its phase ordering dynamics in two dimensions in numerical simulations. Imposing a local constraint on the dynamics has the surprising effect of speeding up the phase ordering process. The system is shown to exhibit a scaling regime characterized by algebraic domain growth, at odds with the logarithmic coarsening of the standard voter model. A phenomenological approach based on cluster diffusion and similar to Smoluchowski ripening correctly predicts the observed scaling regime. Our analysis exposes unexpected complexity in the phase ordering dynamics without thermodynamic potential.

DOI: 10.1103/PhysRevE.87.052114 PACS number(s): 02.50.Ey, 64.60.Ht, 05.50.+q, 89.75.Da

I. INTRODUCTION

How do systems of interacting particles order, and what are the mechanisms by which microscopic interaction generates macroscopic structures? These questions have first been asked in biology [1] and then in condensed matter physics, magnetism, and statistical mechanics, where kinetic ordering dynamics has received considerable attention [2,3]. Ordering processes have more recently also become of interest in interacting agent models of social processes [4,5].

Our understanding of processes out of equilibrium is still limited, and developing a more complete picture is a focus of current research. Processes of kinetic ordering are traditionally addressed in the context of simple lattice models. In condensed matter physics, their dynamics is usually based on the minimization of a thermodynamic potential, coupled to a heat bath and obeying detailed balance. Such models allow for a characterization of different types of ordering. There is a distinction between models with and without a local conservation law. Glauber dynamics [6] and the kinetic Ising model of magnetic systems have no conservation law. Their characteristic length scale grows algebraically with time, $L(t) \sim t^n$, where the coarsening exponent is found to take the value $n = 1/2$ in phenomenological theories [2,3]. In the conserved Kawasaki dynamics [7], on the other hand, one finds $n = 1/3$ [2,3]. This type of dynamics is used to describe alloys or binary liquids. In both models, the coarsening dynamics is driven by surface tension.

A second class of dynamics is defined by systems lacking a thermodynamic potential or energy function. This type of model, frequently based on pairwise interaction, has also been used to study autocatalytic chemical reactions [8], bacterial populations [9], and social dynamics [5,10]. In lattice models with $\mathbb{Z}_2$ symmetry and absorbing states, domain coarsening can proceed in the absence of surface tension, driven by interfacial noise [11,12]. The main representative of this class is the voter model (VM) [13], in which spinlike variables align with the state of a randomly chosen nearest neighbor. This dynamics does not permit a locally conserved quantity, even though global magnetization is conserved in the ensemble. The coarsening dynamics of the VM is algebraic (with $n = 1/2$) in spatial dimension $d = 1$, and logarithmic in $d = d_c = 2$, that is, $L(t) \propto \ln t$ [14,15]. For $d > d_c$, the interfacial noise becomes irrelevant and the infinite system does not order.

The purpose of our work is to investigate the phase-separation dynamics in models of the voter type, but with local conservation of the order parameter. Specifically, we study spin-exchange processes based on interactions of pairs of particles. Similar to the celebrated Schelling model of segregation [4,16,17], such dynamics can be motivated by social processes [5]. This is not the main objective we wish to pursue, however. We aim to systematically work toward a more complete picture of the possible types of ordering dynamics in off-equilibrium particle models. Specifically, we introduce variants of the VM with local conservation laws. While some VMs modified along these lines do not order at all, others show an effective algebraic domain growth. We provide a phenomenological understanding of this behavior invoking a combination of two different mechanisms: (i) a linear instability triggering the formation of compact faceted patterns, and (ii) a process similar to Smoluchowski ripening [18], responsible for domain coarsening in the long-time regime. The latter occurs through cluster coalescence driven by surface diffusion and follows an algebraic law $L(t) \sim t^{1/5}$. Interestingly, imposing the local constraint does not slow down the dynamics, but speeds it up relative to the logarithmic ordering of the standard unconstrained VM [19].

II. MODEL DEFINITIONS

As in the standard voter model, we consider N binary variables $s_i \in \{+1, -1\}$ defined on sites i of a d-dimensional lattice. In the standard voter model at each time step one spin i is selected at random and then assumes the state of a randomly

*caccioli@santafe.edu
†luca.dallasta@polito.it
‡tobias.galla@manchester.ac.uk
§t.c.rogers@bath.ac.uk

chosen neighbor. This can be thought of as a process of opinion dynamics, where each agent can have one of two possible opinions. If chosen for (potential) update, an agent adopts the opinion of one of his neighbors (chosen at random).

The model we consider here is defined by the following update rule:

(i) At each time step we select a pair of two neighboring sites i, j at random.

(ii) If $s_i = s_j$, no changes are made and the dynamics moves to the next time step, i.e., goto (i) (time is incremented by $1/N$).

(iii) If $s_i \neq s_j$, then for each of the two sites one of their remaining neighbors is chosen, i.e., $k \in \partial i \setminus j$ and $\ell \in \partial j \setminus i$, where ∂i denotes the set of neighbors of i. If $s_\ell = s_i$ and $s_k = s_j$, then the spins s_i and s_j are exchanged, and time is incremented. Goto (i).

More compactly, and assuming the two spins chosen for potential update are i and j, and that $s_i \neq s_j$, the probability with which the two spins are exchanged can be written as

$$R_{ij}^{s_i s_j} = \frac{1 - s_i h_{i\setminus j}}{2} \frac{1 - s_j h_{j\setminus i}}{2}, \qquad (1)$$

where $h_{i\setminus j} = \frac{1}{2d-1} \sum_{k\in\partial i\setminus j} s_k$ and where ∂i is the neighborhood of i.

In the language of social dynamics, an update step corresponds to two neighboring individuals of different types exchanging their positions on the d-dimensional lattice. This is in the spirit of Schelling's model of segregation, see for example [4], in which agents of two different types may exchange positions on a regular lattice, subject to certain dynamical rules and—unlike in our model—also allowing long-range interactions. The underlying principle of Schelling's model is that an agent prefers to be surrounded by other agents of his type.

In our model, once a pair of neighbors i and j of different types ($s_i \neq s_j$) has been chosen for potential exchange, they each assess the state of one of their neighbors, chosen at random and excluding the partner with which potential exchange may occur. Say the chosen neighbor of i is k and that of j is ℓ. As in Schelling's model, agents of a given type prefer to be surrounded by agents of the same type. So an exchange of i and j occurs if (i) $s_\ell = s_i$, i.e., the potential new neighbor of i after the exchange is in state s_i, and (ii) if $s_k = -s_i$, i.e., the "old" neighbor of i is in the state opposite to that of i. If these two conditions are fulfilled, then spin i's perceived situation, based on the sampling of one random neighbor in his present and potential new neighborhood, respectively, strictly improves by virtue of the exchange. Given that we have already assumed $s_j = -s_i$, the same is true for agent j based on the same sampling. Thus, exchanges occur if and only if both agents chosen for potential exchange (strictly) improve their perceived situation.

III. COARSENING DYNAMICS, SCALING, AND CLUSTER SIZE DISTRIBUTION

A. Coarsening dynamics

We consider unbiased random initial conditions in $d = 2$ dimensions. The temporal behavior of the density of interfaces (neighboring pairs of opposing spins) $\rho(t)$, shown in Fig. 1(a), reveals a very slow initial dynamical regime, in which clusters

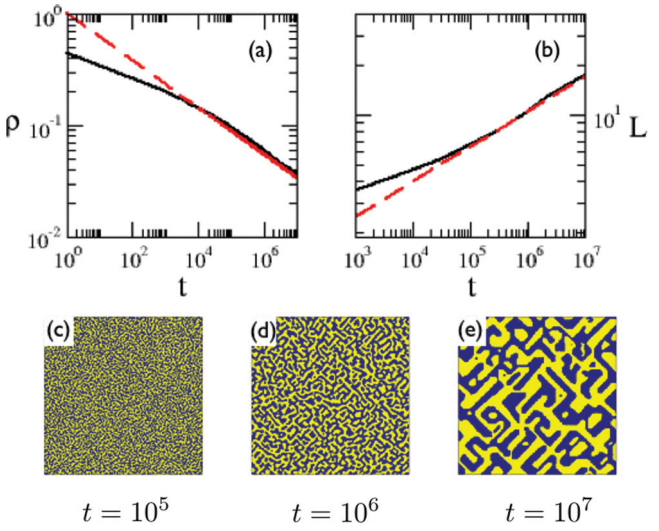

FIG. 1. (Color online) Voter model with microscopically conserved dynamics. Panels (a) and (b) show the time evolution of the density of interfaces and correlation length, respectively; (c)–(e) snapshots of the kinetic ordering process. Dashed lines in (a) and (b) indicate algebraic growth laws with exponent 0.21. Data are from simulations of a 500×500 system.

of spins with the same orientation are formed. At long times the system enters a regime of algebraic coarsening, in which the density of interfaces decays according to $\rho(t) \sim t^{-x}$. This behavior is similar to that seen in curvature-driven phase separation, and in contrast to the usual VM in $d = 2$, which exhibits logarithmic coarsening. In this dynamic scaling regime, the system has a single characteristic length scale, $L(t)$, and the order-parameter correlation function assumes a scaling form $C(r,t) = f[r/L(t)]$. The typical length scale can be extracted from the first zero of the correlation function, $C(r,t)$, and is found to grow algebraically, $L(t) \propto t^n$; see Fig. 1(b). From our data, the coarsening exponent is found to be $x \simeq n \simeq 0.21$, and therefore it is different from the standard exponent $1/3$ in curvature-driven coarsening with a locally conserved order parameter [2]. Snapshots from simulations of the conserved VM are shown in Figs. 1(c)–1(e); over time, the system develops faceted domains with straight and elongated diagonal boundaries.

B. Scaling of the structure factor

To provide further evidence for the scaling behavior of the model with local microscopic conservation, we show results for the structure factor obtained from numerical simulations in Fig. 2. Data have been obtained from a two-dimensional Fourier transform with respect to the spatial coordinates, and an average over the axes of the lattice has then been performed. The figure shows the structure factor, $S(k)$, rescaled by the typical length scale $L(t)$ and where k is the wave number. The length scale, $L(t)$, is obtained from the first zero of the corresponding correlation function. As seen in Fig. 2, the numerical data support the scaling hypothesis $S(k,t) = L^2 g(kL)$.

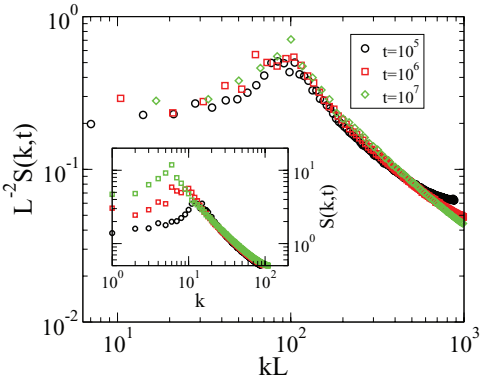

FIG. 2. (Color online) Collapse plot of the structure factor, as obtained from a single run of a 500×500 system. Rescaling of the raw structure factor is by powers of the relevant length scale, $L(t)$, defined in the text. The inset shows the data prior to rescaling.

C. Properties of clusters

We have also investigated the shape of clusters in the conserved voter model. To this end we have, at different times of the dynamics, measured the area, A, and the perimeter, P, of each cluster in the system. Results are shown in Fig. 3. As seen in the upper panel of the figure, one has $A \sim P^2$ for small clusters, indicating a roughly isotropic shape. Large clusters, on the other hand, are long and thin, as also seen in Fig. 1. They show a scaling $A \sim P$. In the lower panel of Fig. 3, we finally plot the rescaled cluster size, A/L^2, versus the rescaled perimeter, P/L, where L is the characteristic length scale obtained from the spatial correlation function. As seen in the figure, the data obtained at different stages of the dynamics collapse well onto one single curve after the rescaling, providing further evidence for the scaling of the system. We point out that similar plots have been considered in the context of other coarsening systems, for example in [20].

IV. RELATION TO KAWASAKI EXCHANGE DYNAMICS

In this section, we briefly relate the VM dynamics with conservation to traditional Kawasaki update dynamics in spin systems. It is useful here to first compare the standard VM with the conventional zero-temperature Glauber dynamics of the Ising model.

In Glauber dynamics [6], one spin i is chosen at random at each step of the dynamics, and then its local field $h_i = (2d)^{-1} \sum_{j \in \partial i} s_j$ is computed. Then, at zero temperature, and if $h_i \neq 0$, the spin s_i is aligned with the field, i.e., s_i is set to take the value $\mathrm{sgn}[h_i]$. If $h_i = 0$, then s_i takes a random state, i.e., $s_i = \pm 1$, each with probability $1/2$.

The dynamics of the conventional VM is similar [13], the only difference being that a flip of spin i (once selected for potential update) occurs with probability $(1 - h_i s_i)/2$. Instead of introducing a local field h_i, the update can be performed taking the value of one randomly chosen neighbor of i.

We now turn to spin dynamics with conservation and compare standard Kawasaki dynamics (at $T = 0$) and the dynamics of the VM with local conservation. In standard Kawasaki dynamics [7] at zero temperature, two neighboring spins i and j are chosen for potential exchange, and their

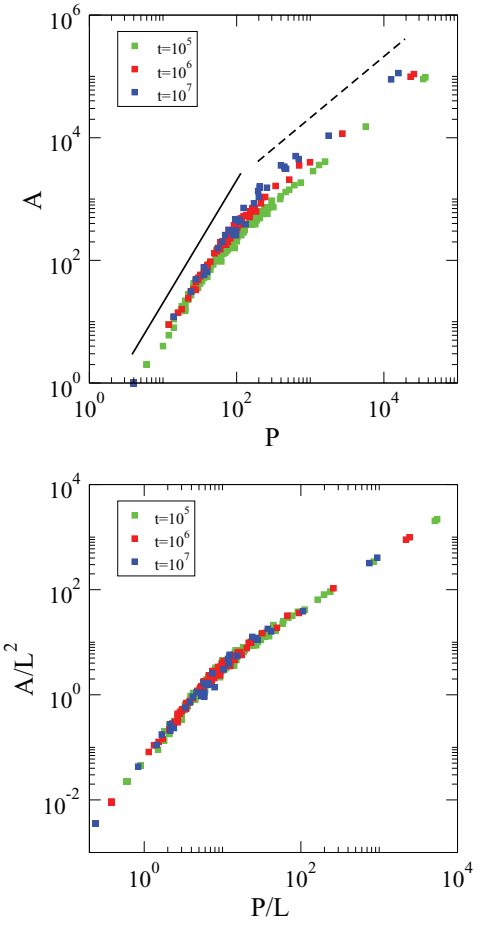

FIG. 3. (Color online) Upper panel: Scatter plot showing the perimeter P of clusters as a function of their area A. Each symbol represents one cluster. Simulation results are from one run of a system of size 500×500. Lines indicate relations of the type $A \sim P^2$ (solid) and $A \sim P$ (dashed), respectively. Lower panel: Same data rescaled by appropriate powers of the length scale $L(t)$ obtained from the spatial correlation function.

local fields $h_i = (2d)^{-1} \sum_{k \in \partial i} s_k$ and $h_j = (2d)^{-1} \sum_{\ell \in \partial j} s_\ell$ are computed. If $s_i = s_j$, exchange has no effect. If $s_i = -s_j$ and if $(h_i - h_j)(s_i - s_j) < 0$, the exchange is carried out, and if $(h_i - h_j)(s_i - s_j) > 0$, the exchange is not carried out. If $h_i = h_j$, then the exchange is carried out with probability $1/2$.

A conserved VM which relates to the Kawasaki dynamics as the conventional VM relates to the kinetic Ising model can be obtained by replacing the fields h_i and h_j in the Kawasaki dynamics as just described by the state of one randomly chosen neighbor of i and j, respectively. This leads to the update rates sketched in Fig. 4. In particular, the resulting model exhibits bulk diffusion, and we find that only partial ordering occurs at long times, with the density of defects settling to a value just below $\rho = 0.4$; see the lower right-hand panel of Fig. 4.

The model discussed in Sec. II is obtained by prohibiting the transitions that occur with rate $1/2$ in Fig. 4, i.e., by only allowing spin exchanges if *both* involved agents strictly improve their perceived neighborhood. In terms of the partial local fields $h_{i\setminus j} = (2d-1)^{-1} \sum_{k \in \partial i \setminus j} s_k$ and $h_{j\setminus i} = (2d-1)^{-1} \sum_{\ell \in \partial j \setminus i} s_\ell$, an exchange of spins i and j (once selected

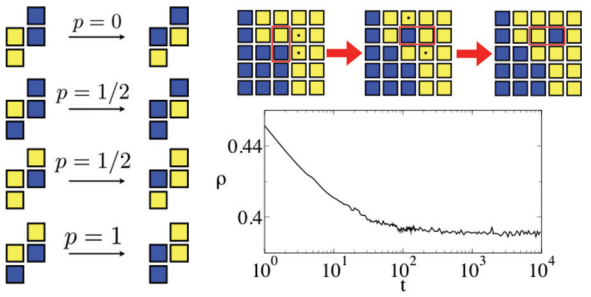

FIG. 4. (Color online) Left: Probabilities for spin exchanges in a conserved VM directly inspired by $T = 0$ Kawasaki dynamics (see text). The figure shows the probability of exchange of the two spins in the middle row of each configuration given that the indicated neighbors are chosen. Upper right: This model allows for bulk diffusion (both indicated updates occur with rate 1/2). Lower right: Density of interfaces as a function of time (average of five runs for a system of size 200 × 200).

for potential update, and given that they are in different states) occurs with probability $(1 - h_{i\setminus j}s_i)/2(1 - h_{j\setminus i}s_j)/2$.

V. PATTERN FORMATION AND MEAN-FIELD APPROACH

Unlike standard VMs, the stochastic dynamics of the model defined in Sec. II cannot be solved exactly due to the nonlinearity of the transition rates. Following classical approaches [3], we neglect correlations between different sites and derive mean-field evolution equations replacing the average of products of spins $\langle s_i \cdots s_j \rangle$ by the product of their averages $\langle s_i \rangle \cdots \langle s_j \rangle$. We will use the variable φ_i to identify the mean-field approximation of the average spin value $\langle s_i \rangle$. In a continuous-time limit, the evolution equation for the local magnetization φ_i becomes

$$\dot{\varphi}_i = \frac{2}{d} \sum_{j \in \partial i} \left[\frac{1-\varphi_i}{2} \frac{1+\varphi_j}{2} R_{ij}^{-+} - \frac{1+\varphi_i}{2} \frac{1-\varphi_\ell}{2} R_{ij}^{+-} \right], \quad (2)$$

resulting in a lengthy expression on the right-hand side, reported in detail in the Appendix. These mean-field equations satisfy the conservation law $\sum_i \dot{\varphi}_i = 0$. The mean-field description can be used to explain the process of pattern formation. Linearizing (2) around the homogeneous solution $\varphi_i \equiv 0 \; \forall i$, one finds

$$\dot{\varphi}_i \propto -\left[\nabla^4 + \frac{1}{d} \nabla^2 \right] \varphi_i, \quad (3)$$

where $\nabla^2 \varphi_i$ is the (lattice) Laplacian. The present model is therefore characterized by a linear instability of type II in the Cross-Hohenberg classification [21] with a band of unstable wave numbers $0 < k < 1/\sqrt{d}$ with maximum growth rate at $k_{\max} = 1/\sqrt{2d}$ (see the Appendix). A linear instability generated by terms of the type as in (3) is typical of coarsening with conserved dynamics, described by the Cahn-Hilliard equation [2]. These terms have a different origin in our model, however. In the Cahn-Hilliard equation, the term proportional to $-\nabla^2 \varphi$ comes from linearizing the thermodynamic potential; in the present model it is instead generated dynamically by exclusion of spin j from the sampling of i's neighborhood and i from the sampling of j's neighborhood. This restriction prevents *bulk diffusion*, i.e., the migration of isolated defects, which is present in the Kawasaki spin-exchange dynamics even at $T = 0$ [3]. The influence of the restriction becomes progressively less important in higher dimensions, and the linear instability is expected to disappear for $d \to \infty$. If we remove the site restriction, only the surface diffusion term, $-\nabla^4 \varphi$, survives in Eq. (3), and phase separation does not occur [3].

Although the mean-field approach describes the pattern formation process qualitatively to some extent, it does not capture the correct long-time coarsening regime. This is not surprising. In the example of the standard VM, the mean-field dynamics is simply given by the diffusion equation, and it does not capture the essential features of the dynamics in low spatial dimensions (e.g., $d = 2$), where the fluctuations due to multiplicative interfacial noise are relevant. The conserved VM we discuss here is more complicated, nevertheless the differences between the dynamics of the original microscopic model and the mean-field equations can again be traced back to the discreteness of the degrees of freedom, i.e., to multiplicative noise.

To interpolate between the model described in Sec. II and the mean-field dynamics, we have considered a modified model in which each lattice site contains Ω spins, similar to what was proposed in [22]. In a given update step, a spin interacts with randomly chosen spins in the neighboring sites, following the microscopic rules of the conserved VM. In models of this type, each site is effectively a population of Ω spins interacting with neighboring populations, and such models are frequently referred to as "metapopulation" models. For $\Omega = 1$, one recovers the conserved VM as defined in the main paper. For $\Omega \to \infty$, the dynamics is deterministic and given by the above mean-field equations; see the Appendix for further details.

The data in Fig. 5 show that for Ω large but finite, the temporal behavior is very similar to the predictions of the mean-field equations in an initial brief coarsening regime governed by surface diffusion (also referred to as "bidiffusion" [3]) and with algebraic coarsening with $n \approx 1/4$. Then the pattern formation process takes place and the dynamics finally reaches a structured configuration of patterns, with only a slow

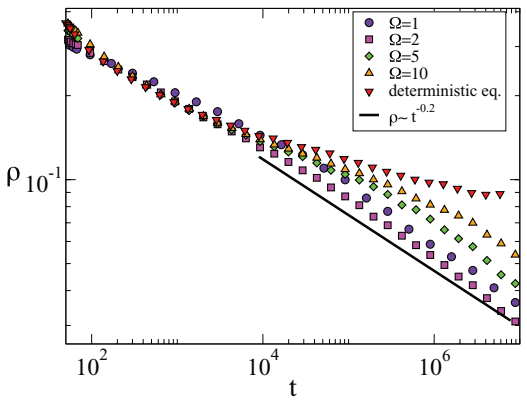

FIG. 5. (Color online) Interface density from a numerical integration of the mean-field dynamics, Eq. (2), and from the microscopic model with Ω spins per site. Data are from single simulation runs of a system of size 200 × 200.

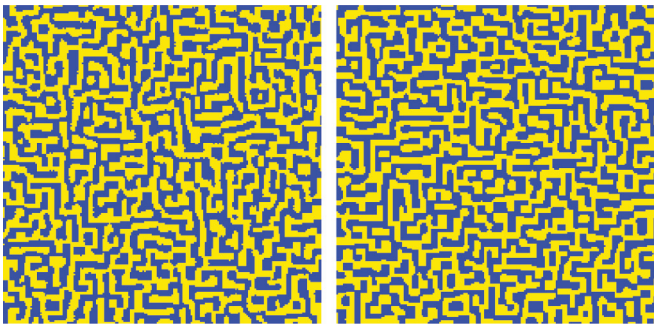

FIG. 6. (Color online) Left: Configuration of the metapopulation conserved voter model with $\Omega = 11$ spins per lattice site (taken at $t = 10^3$ in a system of size 200×200). Right: Configuration obtained from the mean-field dynamics (taken at $t = 10^3$).

further coarsening process or potentially none. Considering the case of small $\Omega \approx 1$, instead, the system develops an algebraic coarsening regime with exponent $n \simeq 0.2$, which persists in the long-time regime. We will discuss the phenomenological behavior of the metapopulation model in more detail in the next section.

VI. PHENOMENOLOGY OF THE METAPOPULATION MODEL

As shown in Fig. 5, the coarsening of the model with $\Omega > 1$ is quite distinct from that of the original model with only one spin per site. This is also seen in Fig. 6, where we show a configuration obtained from the metapopulation model, and which should be compared with those of the model with $\Omega = 1$ shown in Fig. 1. Clusters appear to have predominantly diagonal interfaces in the model with $\Omega = 1$, whereas interfaces are mostly aligned with the lattice directions in the model with $\Omega > 1$. Structures obtained from a numerical integration of the mean-field dynamics at intermediate times are consistent with those obtained from the model with $\Omega > 1$; see Fig. 6. The different orientation of domains observed in the two models can intuitively be traced back to mechanisms by which domains tend to maximize their mobility and ability to grow at the boundaries, as we will detail next.

A. Coarsening dynamics with $\Omega = 1$

For $\Omega = 1$, straight horizontal and vertical boundaries are frozen, since no spin at the boundary is able to find two neighbors of a sign different from its own. Diagonally oriented domains, in contrast, have a much higher mobility at the boundary, and this allows domains to grow. Additionally, two different square (or rectangular) domains of the same spin orientation can merge in the model with $\Omega = 1$ if they share a common corner; see Fig. 7 for a simulation example. This can generate a diagonally oriented domain. It should be noted that a single cluster of up-spins in a sea of down-spins may develop straight domain boundaries eventually. This is what happens to the isolated cluster shown in the rightmost panel of Fig. 7, and a similar phenomenon can be seen for some of the small clusters in Fig. 1 upon closer inspection.

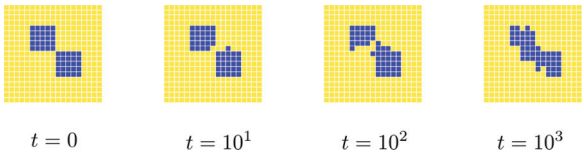

FIG. 7. (Color online) Dynamics of two clusters in the model with $\Omega = 1$. Initially the two clusters "touch" each other at one corner and then merge into one cluster with mostly diagonal orientation. Data are from a single simulation run of a system of size 20×20.

We speculate that isolated clusters of one type of spin may form vertical and horizontal boundaries when surrounded by a much larger sea of spins of the opposite sign. This is corroborated by the configuration shown in Fig. 8, generated from an initial condition in which spins are in one state with probability 80% and in the other with probability 20%. As seen in the figure, isolated clusters of the minority type then tend to form horizontal and vertical boundaries. On the other hand, diagonal interfaces may develop when the cluster size is comparable to the size of the surrounding domain of spins of the opposite type; see Fig. 9 for an example.

B. Coarsening dynamics with $\Omega > 1$

When $\Omega > 1$, on the other hand, diagonal interfaces are not needed in order for domains to grow. In this case, the interface between two different domains consists of a layer of nodes with intermediate net magnetization (i.e., the population of Ω particles residing at such nodes is partly made up of up-spins and partly of down-spins). This provides a "cushion" between different domains, and is sufficient to guarantee mobility even at straight vertical or horizontal domain boundaries. See Fig. 10 for an example in which two clusters, separated by an intermediate layer of cells in a mixed state, merge.

It is also interesting to note an apparent nonmonotonicity of the interface density as a function of Ω at a sufficiently large fixed time (say $t = 10^5$) in Fig. 5. One finds that the density of defects decreases when going from $\Omega = 1$ to 2, and that it then increases again as Ω is increased further. This may look surprising at first, but a possible qualitative explanation can be given once one realizes that the dynamics at $\Omega = 1$ is different from that at $\Omega > 1$ (taking out the curve for $\Omega = 1$ in the figure leads to a monotonically increasing density as a function of Ω). For $\Omega > 1$, the interaction between domains

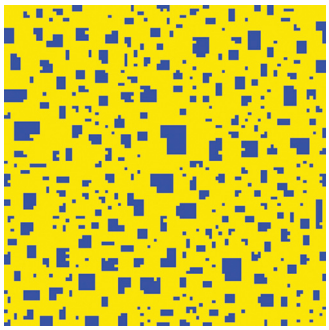

FIG. 8. (Color online) Configuration of a 100×100 system ($\Omega = 1$) at time $t = 10^5$, started from a random initial condition in which each spin is in state $+1$ (dark squares) with probability 20%.

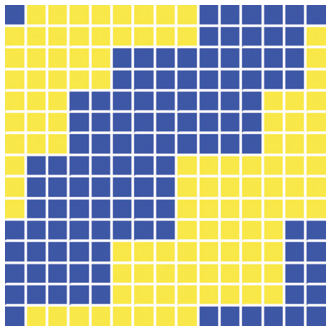

FIG. 9. (Color online) Final frozen configuration of a small system with 15×15 spins ($t = 10^5$), started from random initial conditions, in which each spin is equally likely to be up or down.

of the different phases occurs through a layer of intermediate states, as explained above, while this is not the case for $\Omega = 1$.

Finally, the following remarks may help to further relate the model with $\Omega = 1$, the metapopulation model ($1 < \Omega < \infty$), and the mean-field limit ($\Omega \to \infty$). At finite $\Omega > 1$ and at intermediate times when domains have formed, but when they are still much smaller than the typical width of the "cushion" of intermediate states, one might naively expect a dynamics similar to mean field. In this regime, the dynamics is dominated by this intermediate layer. At larger times, domains will have outgrown the typical size of the intermediate layer, and one then enters a dynamical regime similar to that of the model with $\Omega = 1$ (for which there are no intermediate zones of mixed up- and down-spins). This is indeed what we see in Fig. 5: for $\Omega > 1$ we observe a preasymptotic regime were domain growth essentially follows the scaling of the mean-field prediction before entering the asymptotic limit with the same growth of the $\Omega = 1$ model. The length of the preasymptotic regime increases with Ω, and becomes the true asymptotic limit for $\Omega \to \infty$.

VII. COARSENING BY CLUSTER DIFFUSION

At this point it is clear that the observed asymptotic coarsening regime in Fig. 1 is an intrinsic effect of individual discreteness, and that it cannot be captured by simple mean-field equations. Instead we follow a phenomenological

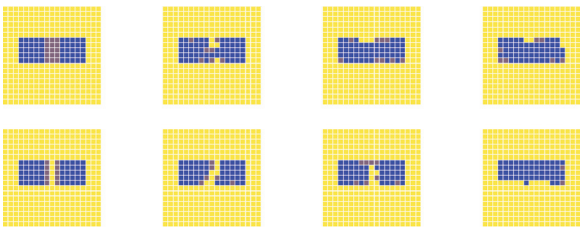

FIG. 10. (Color online) Dynamics of two clusters in the model with $\Omega = 2$. In this model each site can be in one of three states (both spins up, both spins down, or one up and one down). Cells in the intermediate state are marked brown (gray). Data are from two separate simulation runs of a system of size 20×20, started from two different initial conditions. In both cases the two clusters, which are initially separated and have straight interfaces, merge eventually.

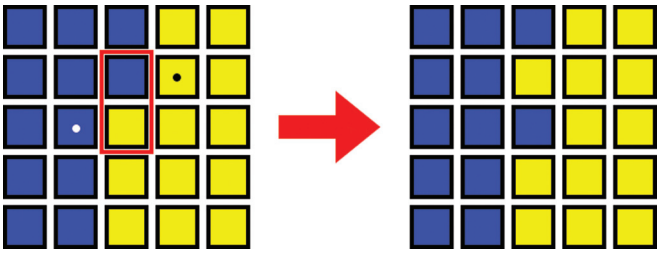

FIG. 11. (Color online) Periphery diffusion: The exchange process of the two spins marked by the red (gray) frame, along with their respective neighbors (marked by dots), leads to a rearrangement of kinks at the interface between two clusters. This may result in a diffusion dynamics of the center of mass of clusters (cluster diffusion).

approach, relating to a phenomenon known in material science as Smoluchowski ripening [18], to obtain further insight into the process of cluster aggregation. In the absence of bulk diffusion, we can exclude Ostwald ripening [23], therefore we expect a slow coarsening process, with $n < 1/3$. Horizontal and vertical domain walls are blocked, while other interfaces can still move by means of a process known as "periphery diffusion," which is a slow diffusional movement of kinks on the boundary of a domain (see the illustration in Fig. 11). This movement causes a slow effective displacement of the center of mass of the clusters, i.e., an effective *cluster diffusion* process. Larger clusters move more slowly because the effective diffusion coefficient of the cluster depends on the ratio between the surface and the volume of the clusters. The form of the resulting diffusion coefficient of clusters has been derived in the literature; see, e.g., [24]. To move the center of mass of a cluster by a distance δ_c in two dimensions, we need order L^2 spins to move by the same distance. This corresponds to a single spin moving over a distance $\delta_p \propto L^2 \delta_c$. On the other hand, the rate at which moves of the center of mass of a cluster occur is proportional to that of diffusion events on its surface, i.e., $\Gamma_c \propto \Gamma_p L$. Given that the single spin diffusion coefficient is $D_p \propto \delta_p^2 \Gamma_p$, we obtain that the diffusion coefficient of a cluster of typical scale L decays as $D_c(L) \propto L^{-3}$.

To find the coarsening exponent, we next consider the temporal evolution of the average cluster size by means of the Smoluchowski equation for cluster coagulation processes. This mean-field approach is usually considered qualitatively correct also in two dimensions. Kang and Redner [25] have shown that the upper critical dimension is $d_c = 2$. We therefore expect logarithmic corrections at most. We follow the derivation proposed by Kandel [26] and introduce the size (area) of a cluster in d dimensions, s. The time-dependent density of clusters of size s per lattice site is denoted by $P(s,t)$ [27]. One then finds the following scaling relation in the long-time limit [26]:

$$P(s,t) = t^{-\alpha} f[s/s_{\mathrm{av}}(t)], \tag{4}$$

where the average cluster size $s_{\mathrm{av}}(t) = \sum_s s P(s,t) / \sum_s P(s,t)$ scales as $s_{\mathrm{av}}(t) \sim t^{\beta}$. The scaling exponents are predicted to be $\alpha = 2/(\zeta + 1)$ and $\beta = 1/(\zeta + 1)$, where ζ characterizes the scaling of the diffusion constant of clusters, with the cluster size, $D_c(s) \sim s^{-\zeta}$ [26]. The scaling of Eq. (4) is confirmed by simulations of the microscopic model, see Fig. 12, adding weight to the hypothesis that a process similar to

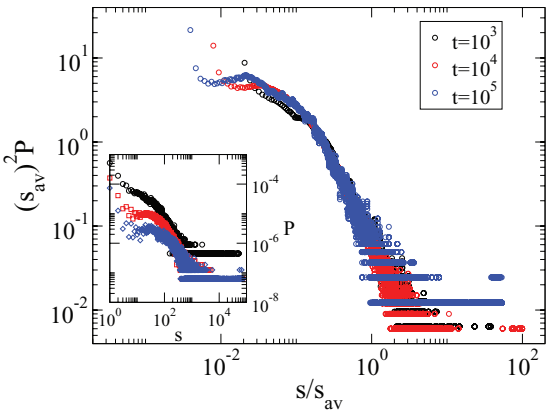

FIG. 12. (Color online) Scaling behavior of the cluster-size distribution $P(s,t)$. The main panel shows the collapse plot obtained using the predicted scaling relation Eq. (4); the inset shows the raw data for $P(s,t)$. Data are from 10 runs of a system of size 400×400 (running average performed to smoothen the data).

Smoluchowski ripening is at work in our system. In the present case, we have $D_c(L) \sim L^{-3}$, i.e., $\zeta = 3/2$. Therefore, we expect that the asymptotic behavior of the microscopic model is characterized by a coarsening regime $s_{\rm av} \sim t^{2/5}$. Given that L is the unique length scale, the hypothesis of Smoluchowski ripening leads to $L \sim t^n$ with $n = \beta/d = 1/5$. The data shown in Fig. 1 are consistent with this phenomenological prediction. We note, however, that the faceted configurations shown in Fig. 1 differ from those seen in physical systems undergoing Smoluchowski ripening [28]. In these systems, one species of particles is frequently more abundant than the other, which may explain the difference in the resulting structures [29].

VIII. MODIFIED DYNAMICS

A. Local dynamics without site exclusion

In this section, we ask whether the complex behavior observed for this dynamics persists if we do not exclude spin j when k is selected, and i when ℓ is chosen. That is, we consider a model in which one first chooses two random neighboring sites i and j and then two spins $k \in \partial i$ and $\ell \in \partial j$. As seen in Fig. 13, this modification has a significant effect on the

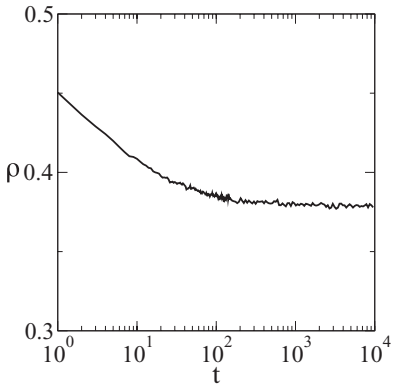

FIG. 13. Interface density for the voter model with conserved dynamics and interaction with all neighbors. Simulation results are from five runs of a system of size 200×200.

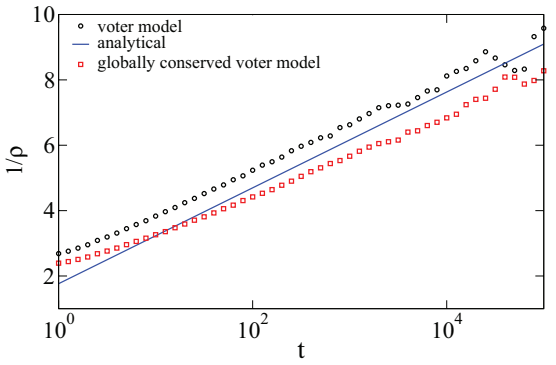

FIG. 14. (Color online) Interface density for the voter model with conserved dynamics and long-range interaction (see text). The upper curve shows simulation results for the standard voter model, while the lower curve shows results for the voter model with long-range interaction. The solid line represents the approximative asymptotic analytical result $\rho(t) = \pi/\ln(256t^2)$ obtained for the density of reactive interfaces in the standard voter model in [15]. Simulation results are from one run of a system of size 1000×1000.

dynamics. The system no longer coarsens; instead, the density of interfaces levels off at a density of defects, ρ, just below 0.4. This is similar to what was seen in the conserved VM directly inspired by zero-temperature Kawasaki spin exchange (see Fig. 4). Both models allow bulk diffusion and show only partial ordering at long times. The possibility of bulk diffusion on the model without site exclusion is easy to see, given that any two neighboring spins i and j that are in different states ($s_i \neq s_j$) can exchange positions in principle, namely if j is chosen as the additional neighbor of i, and i as that of j.

B. Voter model with long-range interaction and global conservation law

To determine if the modified scaling behavior we observe is genuinely an effect of local (microscopic) conservation, as opposed to conservation *per se*, we considered a version of the dynamics with conservation only at a global level, specifically a variation of the voter model with global conservation of the magnetization, but with long-range interaction. At each step of the dynamics, two spins i and j are chosen at random in the system (i.e., i and j need not be nearest neighbors). If the two spins are in different states, one neighbor k of i and one neighbor ℓ of j are chosen at random. The dynamics is then carried out as described above, i.e., the states of spins i and j are exchanged if $s_k = s_j$ and $s_\ell = s_i$.

Results are shown in Fig. 14. The simulations confirm that the coarsening in this long-range model with conservation is logarithmic, similar to what is seen in the standard voter model without conservation law. These findings are in line with earlier work indicating that conservation laws at long range do not affect the coarsening dynamics of nonconserved models [30].

IX. CONCLUSIONS

We have put forward a voterlike model with strict microscopic conservation of magnetization. The spin-exchange rule introduces nonlinearities that turn the logarithmic growth of the standard VM into an algebraic coarsening process, driven

by diffusion at the surfaces of clusters and by coalescence of clusters, similar to what is known as Smoluchowski ripening. Simulation results are consistent with a growth law $L \sim t^{1/5}$, as predicted by a phenomenological theory. While it is well known that introducing nonlinearities in the update rule of the voter model can restore surface tension and algebraic coarsening [31], the analysis is usually limited to nonconservative processes. Our results on conservative dynamics extend the complexity and variety of interacting particle models out of equilibrium. We also provide a clear understanding of the mechanism by which cluster diffusion and Smoluchowski ripening can be responsible for phase separation in systems lacking a thermodynamic potential. This can be relevant for a more complete classification of nonequilibrium processes in low-dimensional systems, and could find application in agent-based modeling, for instance in the study of mobility and segregation in social sciences.

ACKNOWLEDGMENTS

T.G. is supported by a RCUK (EP/E500048/1). T.G. and T.R. acknowledge support by EPSRC (EP/I005765/1 and EP/H02171X/1). L.D.A. acknowledges support by EU FET Open 265496 and FIRB Project RBFR10QUW4. F.C. was supported by the National Science Foundation under Grant No. 0965673.

APPENDIX: MEAN-FIELD DYNAMICS

1. Derivation

The purpose of this appendix is to derive the rate equation [see Eq. (2)],

$$\dot{\varphi}_i = \frac{2}{d}\sum_{j\in\partial i}\left\{\frac{1-\varphi_i}{2}\frac{1+\varphi_j}{2}R_{ij}^{-+} - \frac{1+\varphi_i}{2}\frac{1-\varphi_j}{2}R_{ij}^{+-}\right\}, \tag{A1}$$

for the field φ_i, which in the model with Ω particles per site denotes the expected magnetization in site i. As we will see below, this description will be accurate in the limit $\Omega \to \infty$. We have introduced

$$R_{ij}^{s_i s_j} = \frac{1-\varphi_i h_{i\setminus j}}{2}\frac{1-\varphi_j h_{j\setminus i}}{2}, \tag{A2}$$

where $h_{i\setminus j}$ defines the local field

$$h_{i\setminus j} = \frac{1}{2d-1}\sum_{k\in\partial i\setminus j}\varphi_k. \tag{A3}$$

To understand Eq. (A1) above, consider the model with a finite number of Ω spins per site. Each lattice site is taken to contain a population of Ω spins. In a given update, a spin interacts with randomly chosen spins in the neighboring sites, following the microscopic rules of the conserved VM, as described in Sec. II:

(i) At each time step we select a pair of two neighboring sites i,j at random, and one random spin s_i^a in site i and one random spin s_i^b in site j ($a,b \in \{1,\ldots,\Omega\}$).

(ii) If $s_i^a = s_j^b$, no changes are made and the dynamics moves to the next time step, i.e., goto (i) [time is incremented by $1/(\Omega N)$].

(iii) If $s_i^a \neq s_j^b$, then for each of the two sites one of their remaining neighbors is chosen, i.e., $k \in \partial i \setminus j$ and $\ell \in \partial j \setminus i$. One then picks random spins s_k^c and s_ℓ^d in k and ℓ, respectively, with $c,d \in \{1,\ldots,\Omega\}$. If $s_\ell^d = s_i^a$ and $s_k^c = s_j^b$, then the spins s_i^a and s_j^b are exchanged, and time is incremented. Goto (i).

We next calculate the *expected* change of magnetization in a given site i per *microscopic* step. The probability that the spin-pair (i,j) is chosen for potential update in this particular microscopic step is $1/(dN)$, if $N = L^d$ is the number of spins in the system (there are then dN nonordered pairs of neighbors). The first term on the right-hand side (RHS), $\frac{1-\varphi_i}{2}\frac{1+\varphi_j}{2}R_{ij}^{-+}$, is then the probability that one of the Ω spins in site i changes its sign from $-$ to $+$ (in exchange with a spin of the opposite sign in site j). In this case, the magnetization in site i changes by $+2/\Omega$. The second term on the RHS of the sum in Eq. (A1) describes the opposite process: $\frac{1+\varphi_i}{2}\frac{1-\varphi_j}{2}R_{ij}^{+-}$ is the probability that one of the Ω spins in i changes from $+$ to $-$, given that the pair (i,j) is selected for update. If an exchange of this type occurs, the magnetization in i changes by $-2/\Omega$.

The *expected* change of magnetization in site i per *microscopic* time step is hence

$$\langle\Delta m_i\rangle = \frac{1}{dN}\frac{2}{\Omega}\sum_{j\in\partial i}\left\{\frac{1-\varphi_i}{2}\frac{1+\varphi_j}{2}R_{ij}^{-+} - \frac{1+\varphi_i}{2}\frac{1-\varphi_j}{2}R_{ij}^{+-}\right\}. \tag{A4}$$

Given that one microscopic time step corresponds to $\Delta t = 1/(N\Omega)$ units of time, we find

$$\dot{\varphi}_i = \lim_{\Omega\to\infty}\frac{\langle\Delta m_i\rangle}{\Delta t} = \frac{2}{d}\sum_{j\in\partial i}\left\{\frac{1-\varphi_i}{2}\frac{1+\varphi_j}{2}R_{ij}^{-+} - \frac{1+\varphi_i}{2}\frac{1-\varphi_j}{2}R_{ij}^{+-}\right\}, \tag{A5}$$

which is Eq. (A1) above.

2. Further simplification

The expression for R_{ij}^{+-} can be written as

$$\begin{aligned}
R_{ij}^{+-} &= \frac{1}{4}\left(1+\frac{1}{2d-1}\varphi_j - \frac{1}{2d-1}\sum_{l\in\partial i}\varphi_l\right)\\
&\quad\times\left(1-\frac{1}{2d-1}\varphi_i + \frac{1}{2d-1}\sum_{k\in\partial j}\varphi_k\right)\\
&= \frac{1}{4}\left(1+\frac{1}{2d-1}\varphi_j - \frac{2d}{2d-1}(\varphi_i+\nabla^2\varphi_i)\right)\\
&\quad\times\left(1-\frac{1}{2d-1}\varphi_i + \frac{2d}{2d-1}(\varphi_j+\nabla^2\varphi_j)\right)\\
&= \frac{1}{4}\left(\frac{2d}{2d-1}\right)^2\left(1-\varphi_i-\nabla^2\varphi_i - \frac{1}{2d}(1-\varphi_j)\right)\\
&\quad\times\left(1+\varphi_j+\nabla^2\varphi_j - \frac{1}{2d}(1+\varphi_i)\right),
\end{aligned} \tag{A6}$$

where the lattice Laplacian is given by $\nabla^2\varphi_i = \frac{1}{2d}\sum_{j\in\partial i}(\varphi_j - \varphi_i)$.

Next we compute

$$\begin{aligned}(1+\varphi_i)(1-\varphi_j)R_{ij}^{+-} &= \frac{1}{4}\left(\frac{2d}{2d-1}\right)^2(1+\varphi_i)(1-\varphi_j)\\ &\times\left(1-\varphi_i-\nabla^2\varphi_i-\frac{1}{2d}(1-\varphi_j)\right)\\ &\times\left(1+\varphi_j+\nabla^2\varphi_j-\frac{1}{2d}(1+\varphi_i)\right)\\ &= \frac{1}{4}\left(\frac{2d}{2d-1}\right)^2(g_i-\nabla^2\varphi_i-f_{ij})\\ &\times(g_j+\nabla^2\varphi_j-f_{ij}),\end{aligned} \tag{A7}$$

where $g_i = 1-\varphi_i^2-\varphi_i\nabla^2\varphi_i$ and $f_{ij} = (1+\varphi_i)(1-\varphi_j)/2d$. By symmetry one then also has

$$\begin{aligned}(1-\varphi_i)(1+\varphi_j)R_{ij}^{-+} = \frac{1}{4}\left(\frac{2d}{2d-1}\right)^2(g_i+\nabla^2\varphi_i-f_{ji})\\ \times(g_j-\nabla^2\varphi_j-f_{ji}).\end{aligned} \tag{A8}$$

Now, $f_{ij}+f_{ji} = (1-\varphi_i\varphi_j)/d$ and $f_{ij}-f_{ji} = (\varphi_i-\varphi_j)/d$, so in total we have

$$\dot{\varphi}_i = \frac{1}{4}\left(\frac{2d}{2d-1}\right)^2\frac{1}{2d}\sum_{j\in\partial i}\left\{A_{ij}+\frac{1}{2d}B_{ij}+\frac{1}{2d^2}C_{ij}\right\}, \tag{A9}$$

where

$$A_{ij} = g_j\nabla^2\varphi_i - g_i\nabla^2\varphi_j, \tag{A10}$$

$$B_{ij} = (\nabla^2\varphi_j-\nabla^2\varphi_i)(1-\varphi_i\varphi_j)+(g_i+g_j)(\varphi_i-\varphi_j), \tag{A11}$$

$$C_{ij} = -(1-\varphi_i\varphi_j)(\varphi_i-\varphi_j). \tag{A12}$$

The sum over j can now be carried out, resulting in terms containing the lattice Laplacian. This gives (all remaining indices are now i and we suppress them in the following)

$$\dot{\varphi} = \frac{1}{16}\left(\frac{2d}{2d-1}\right)^2\left\{\mathcal{A}+\frac{1}{2d}\mathcal{B}+\frac{1}{2d^2}\mathcal{C}\right\}, \tag{A13}$$

where

$$\mathcal{A} = \nabla^2 g\nabla^2\varphi - g\nabla^4\varphi, \tag{A14}$$

$$\mathcal{B} = (1-\varphi^2)\nabla^4\varphi + 4\varphi(\nabla\varphi)^2 + 2[(\nabla\varphi)^2-g]\nabla^2\varphi, \tag{A15}$$

$$\mathcal{C} = (1-\varphi^2)\nabla^2\varphi - 2\varphi\nabla\varphi\nabla\varphi. \tag{A16}$$

3. Linear stability analysis

Linearizing Eq. (A13) about the homogeneous solution $\varphi_i \equiv 0$, one finds that $\mathcal{A} \approx -\nabla^4\varphi$, $\mathcal{B} \approx \nabla^4\varphi - 2\nabla^2\varphi$, and $\mathcal{C} \approx \nabla^2\varphi$. Collecting terms one has

$$\dot{\varphi} \propto -\left[\nabla^4\varphi + \frac{1}{d}\nabla^2\varphi\right]. \tag{A17}$$

After moving to Fourier space, the growth rate of a mode of wave number k is found to be proportional to $\lambda(k) = -k^4 + k^2/d$, and the most unstable mode is found from $d\lambda/dk = 0$ as $k_{\max} = 1/\sqrt{2d}$.

[1] A. M. Turing, Philos. Trans. R. Soc. B **237**, 37 (1952).
[2] A. J. Bray, Adv. Phys. **43**, 357 (1994).
[3] P. L. Krapivsky, S. Redner, and E. Ben-Naim, *A Kinetic View of Statistical Physics* (Cambridge University Press, Cambridge, 2010).
[4] T. C. Schelling, J. Math. Sociol. **1**, 143 (1971).
[5] C. Castellano, S. Fortunato, and V. Loreto, Rev. Mod. Phys. **81**, 591 (2009).
[6] R. J. Glauber, J. Math. Phys. **4**, 294 (1963).
[7] K. Kawasaki, Phys. Rev. **145**, 224 (1966).
[8] R. M. Ziff, E. Gulari, and Y. Barshad, Phys. Rev. Lett. **56**, 2553 (1986).
[9] E. Frey and T. Reichenbach, in *Evolution: From the Planck Epoch to Complex Multicellular Life*, edited by H. Meyer-Ortmanns and S. Thurner (Springer, Heidelberg, 2011), p. 297.
[10] F. Slanina, K. Sznajd-Weron, and P. Przybyła, Europhys. Lett. **82**, 18006 (2008); S. Galam, *ibid.* **70**, 705 (2005); S. Galam and A. C. R. Martins, *ibid.* **95**, 48005 (2011).
[11] I. Dornic, H. Chaté, J. Chave, and H. Hinrichsen, Phys. Rev. Lett. **87**, 045701 (2001).
[12] O. Al Hammal, H. Chaté, I. Dornic, and M. A. Muñoz, Phys. Rev. Lett. **94**, 230601 (2005).
[13] T. M. Liggett, *Interacting Particle Systems* (Springer-Verlag, New York, 1985).
[14] P. L. Krapivsky, Phys. Rev. A **45**, 1067 (1992).
[15] L. Frachebourg and P. L. Krapivsky, Phys. Rev. E **53**, R3009 (1996).
[16] L. Dall'Asta, C. Castellano, and M. Marsili, J. Stat. Mech.: Theor. Exp. (2008) L07002.
[17] T. Rogers and A. J. McKane, J. Stat. Mech. (2011) P07006; Phys. Rev. E **85**, 041136 (2012).
[18] M. von Smoluchowski, Phys. Z. **17**, 585 (1916).
[19] H.-U. Stark, C. J. Tessone, and F. Schweitzer, Phys. Rev. Lett. **101**, 018701 (2008).
[20] A. Sicilia, J. J. Arenzon, A. J. Bray, and L. F. Cugliandolo, Phys. Rev. E **76**, 061116 (2007).
[21] M. Cross and H. Greenside, *Pattern Formation and Dynamics in Non Equilibrium Systems* (Cambridge University Press, Cambridge, 2009).
[22] L. Dall'Asta and T. Galla, J. Phys. A **41**, 435003 (2008); D. I. Russell and R. A. Blythe, Phys. Rev. Lett. **106**, 165702 (2011).
[23] W. Ostwald, Lehrb. Allgemein. Chem. **2**, part 1 (1896).
[24] C. DeW. Van Siclen, Phys. Rev. Lett. **75**, 1574 (1995).
[25] K. Kang and S. Redner, Phys. Rev. A **30**, 2833 (1984).

[26] D. Kandel, Phys. Rev. Lett. **79**, 4238 (1997).
[27] $P(s,t)$ is the number of clusters at time t containing precisely s spins, divided by the total number of spins in the system. We have $\sum_s sP(s,t) = 1$.
[28] P. A. Thiel, M. Shen, D.-J. Liu, and J. W. Ewans, J. Phys. Chem. C **113**, 5047 (2009); C. R. Stoldt *et al.*, J. Chem. Phys. **111**, 5157 (1999).
[29] Biasing the initial condition in our model, we find a very slow coarsening dynamics—clusters do not appear to coalesce for a significant time. It is therefore hard to assess the asymptotic regime in simulations.
[30] A. J. Bray, Phys. Rev. E **47**, 3191 (1993).
[31] L. Dall'Asta and C. Castellano, Europhys. Lett. **77**, 60005 (2007); R. Lambiotte and S. Redner, *ibid.* **82**, 18007 (2008).